The HUGIN AUV Terrain Navigation Module

Kjetil Bergh Ånonsen, Ove Kent Hagen
Norwegian Defence Research Establishment (FFI)
Kjeller, Norway
Email: kjetil-bergh.anonsen@ffi.no

Øyvind Hegrenæs, Per Espen Hagen
Kongsberg Maritime Subsea, AUV Department
Horten, Norway

***Abstract*—Terrain navigation is an attractive method for obtaining submerged position fixes for autonomous underwater vehicle (AUV), based on terrain measurements and a terrain map of the operation area. On-going research at the Norwegian Defence Research Establishment (FFI) has resulted in a real-time terrain navigation module for the Kongsberg HUGIN AUVs, based on a point mass filter (PMF) estimator. This system is now available as an optional module for the HUGIN vehicles, and has recently been delivered to customers. The paper gives an overview of the HUGIN terrain navigation module and its integration with the rest of the HUGIN navigation system. Results from sea trials using a HUGIN 1000 AUV with an EM2040 are presented, demonstrating some of the capabilities of the system.**

I. Introduction

Precise underwater navigation is crucial in a number of marine applications. This paper focuses on navigation of autonomous underwater vehicles (AUVs), although the techniques described can also be used by other types of underwater vehicles.

Most AUV navigation systems are based on inertial navigation. Inertial navigation systems drift off with time, even when velocity aiding is used. In order to allow extended submerged operations, external position updates are needed. As GPS is not available underwater, one is often dependent on acoustic aiding of the vehicle, either from a mother ship or by using underwater acoustic transponders. In order to increase the autonomy [1], [2] of the vehicle and avoid costly pre-deployment of underwater transponders, terrain-based navigation is a favorable alternative. For the methods discussed here it is assumed that a prior bathymetric map database of the area exists. Any sensor that is able to measure the altitude of the vehicle can be used for terrain navigation. Most, if not all, AUVs carry one or more such sensors. The effectiveness of the sensor for this purpose is determined by the swath width of the sensor. A sensor with multiple measurements in each ping, covering a large swath, like a multibeam echo sounder (MBE), leads to faster convergence of the terrain navigation algorithms than a single measurement sensor, like an acoustic altimeter. As an AUV in most cases carries a bathymetric sensor, it is natural to utilize bathymetric information in the navigation of the vehicle.

Over the last few years, a real-time point mass filter (PMF) based terrain navigation system for AUVs has been developed

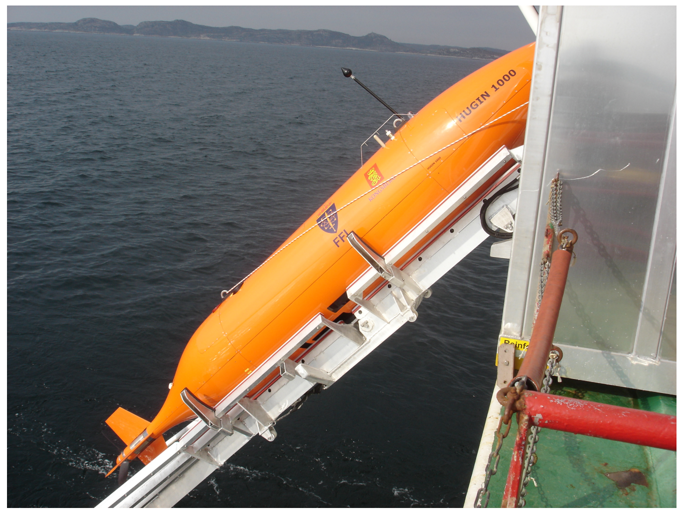

Fig. 1. The HUGIN 1000 HUS seconds before launch from FFI's research vessel H.U. Sverdrup II.

at the Norwegian Defence Research Establishment (FFI), providing the inertial navigation system with position updates based on terrain measurements from different sensors capable of measuring the altitude of the vehicle [3]. Several successful sea trials have been conducted, using different Kongsberg Maritime HUGIN vehicles with different bathymetric sensors [4], [5]. The terrain navigation system is now being offered as an optional module for the HUGIN navigation system, and has been delivered to customers. The system uses the available on-board terrain measuring sensors, usually multibeam echo sounders.

The HUGIN navigation system is a well-proven, robust navigation system, with an extensive toolbox of aiding techniques [6]. The terrain navigation module adds robustness and complements the previously offered aiding techniques. Its success is dependent on the terrain suitability, as a certain degree of terrain variation is needed. In addition, a digital terrain model is needed. The terrain model can be generated from any existing terrain data, including data collected by the vehicle itself during previous surveys. This makes the technique attractive in operations where the same route is surveyed several times, like in route surveys or pipeline

978-0-933957-40-4 ©2013 MTS

inspection surveys. The module also facilitates the use of within-mission terrain data, using terrain data from the early stages of the mission to improve the navigation accuracy when returning to a previously surveyed area later in the mission [5]. After the vehicle is recovered, terrain navigation results can be used in post-processing, in order to improve the final navigation solution, in situations where high navigation accuracy is required.

The outline of the paper is as follows. Section II gives a brief overview of the main HUGIN navigation system. In Section III, the basic mathematical background of Bayesian terrain navigation is reviewed, whereas the HUGIN terrain navigation module is described in Section IV. Section V contains some results from a recent sea trial of the system. Finally, some conclusions and ideas for future work are given in Section VI.

II. The HUGIN Navigation System

A. Overall Design

A description of the basic design of the HUGIN software system is given in [7]. The system consists of:

- A control processor (CP) with a real-time operation system (RTOS), which handles e.g. guidance and control, basic sensors, autonomous decisions and communication.
- A navigation processor (NavP) also with an RTOS. It handles the inertial measurement unit (IMU), and is running the real-time AINS (Aided Inertial Navigation System). In modern HUGIN vehicles, NavP is run as a subprocess on CP, although it was originally run on a dedicated processor.
- A payload processor (PP) with a Win32 compatible OS. It handles all other payload sensors not part of the basic sensor suite.
- A topside HUGIN operator station (HOS) that handles mission planning and monitoring, and communication with HUGIN.

All communication between the CP, PP and NavP processes is based on CORBA (Common Object Request Broker Architecture) [7]. Fig. 2 shows an overview of how the terrain navigation module is deployed on a HUGIN vehicle. The terrain navigation system (TerrP) has been implemented as a plugin on the payload processor (PP). Although the terrain navigation system is fully automatic, a topside user interface called TerrPOS can be used for monitoring and configuration of the system. The TerrP module and its integration with the main navigation system will be more thoroughly described in Section IV.

B. Main Navigation System

A thorough description of the HUGIN navigation system can be found in [6]. The core navigation system (NavP) is based on the output from IMU, using the structure shown in Fig. 3. The measured angular velocity from the gyroscopes and specific force from the accelerometers are integrated using the navigation equations to obtain the vehicle velocity, attitude, depth and horizontal position. The output from the navigation

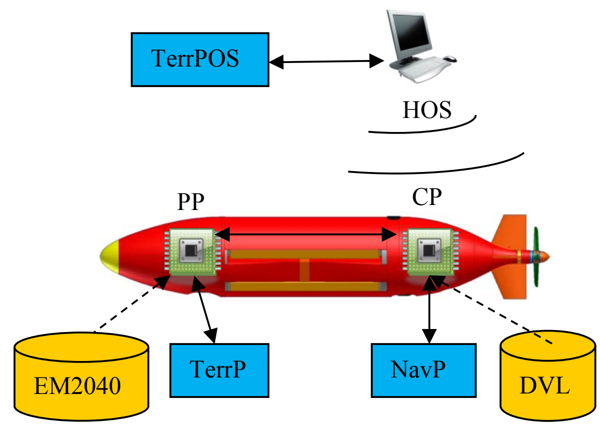

Fig. 2. Overview of NavP and TerrP software modules.

equations are integrated with the different aiding sensors using an error state Kalman filter. The basic aiding sensors are a Doppler velocity log (DVL), an optional magnetic compass, a pressure sensor and a GPS receiver. Due to the modular structure of the system, any other sensor providing horizontal measurement updates can be easily added, the most common being acoustic positioning from the mother ship, combining differential GPS and Ultra-Short Base Line positioning (DGPS + USBL). Another possibility is Underwater Transponder Positioning (UTP), which uses range measurements from pre-deployed transponders to compute position updates [8]. Terrain navigation updates are integrated in the Kalman filter similarly to GPS measurements, using a measurement model based on a linear combination of a first order Gauss-Markov process and white noise, allowing for a possible time correlated bias in the position fix. Such a bias may for example stem from a position bias in the map database.

III. Terrain Navigation Algorithms

In our application, the measurements represent the total water depth at the MBE footprint, i.e. the sum of the AUV depth, calculated from pressure sensor measurements, and the altitude measurements from the MBE. To be able to compare these measurements to the depth values in the map data base, they must be converted to the same vertical datum as the map database, usually mean sea level. Pressure-to-depth conversions for AUVs was thoroughly discussed in [9].

In [10], it was shown how errors in the pressure-to-depth conversion and tide compensation can lead to inaccuracies and errors in the terrain navigation position estimates, and how this problem can be solved by including estimation of the depth bias in the algorithms. In the tests described in this paper, a 2-dimensional estimation model was used. Depth bias issues may however be countered using relative depth profiles, i.e. extracting the mean value from the measured profiles as well as from the map profile.

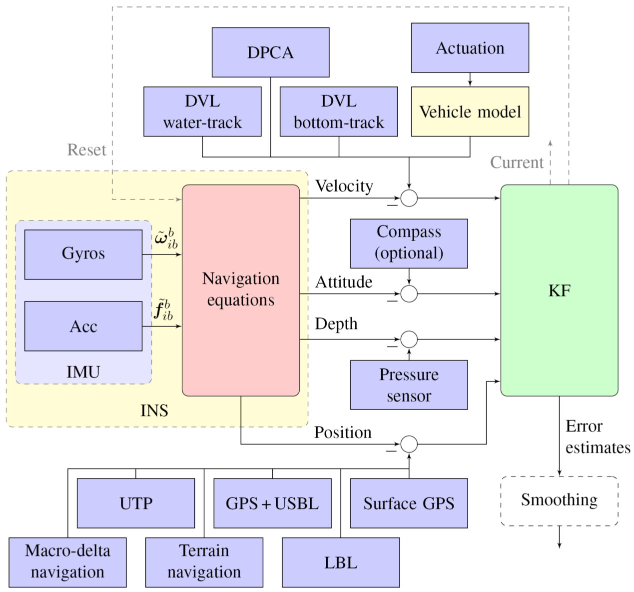

Fig. 3. HUGIN navigation system structure.

A. System Model

We consider the following model for the motion of our AUV,

$$\mathbf{x}_{k+1} = \mathbf{x}_k + \mathbf{u}_k + \mathbf{v}'_k + \mathbf{v}_k, \tag{1}$$

$$\mathbf{v}'_{k+1} = \mathbf{g}(\mathbf{v}'_k) + \mathbf{v}''_k, \tag{2}$$

where $\mathbf{x}_k = (x_N, x_E)^T$ is the AUV position vector, $\mathbf{u}_k$ is the position change calculated from the inertial navigation system, and $\mathbf{v}_k$ and $\mathbf{v}''_k$ are independent white noise sequences. Equation (2) models the strongly correlated error propagation of the inertial navigation system. The system measurement equation is given by

$$\mathbf{z}_k = \mathbf{h}(\mathbf{x}_k) + \mathbf{w}_k, \tag{3}$$

where the bottom depth measurement $\mathbf{z}$ is either a vector or a scalar, depending on the type of sensor considered. For single measurements, such as single beam echo sounders (SBE), the measurements are scalar, whereas for MBEs we have vector measurements. The function $\mathbf{h}(\mathbf{x}_k)$ denotes the true sea depth at position $\mathbf{x}_k$, which has to be estimated by a digital terrain map. The vector $\mathbf{w}_k$ denotes the sensor measurement noise, which is assumed to be white.

In order to simplify the mathematical description of our algorithms, we will express our true position as an offset, $\delta\mathbf{x}$, from the position estimate $\tilde{\mathbf{x}}$ of the inertial navigation system. Our process then becomes

$$\delta\mathbf{x}_k = \mathbf{x}_k - \tilde{\mathbf{x}}_k, \tag{4}$$

$$\begin{aligned}\delta\mathbf{x}_{k+1} &= \mathbf{x}_{k+1} - \tilde{\mathbf{x}}_{k+1} \\ &= \mathbf{x}_k + \mathbf{u}_k + \mathbf{v}'_k + \mathbf{v}_k - \tilde{\mathbf{x}}_k - \mathbf{u}_k \\ &= \delta\mathbf{x}_k + \mathbf{v}'_k + \mathbf{v}_k. \end{aligned}\tag{5}$$

B. Filter model

Due to the computational requirements of the point mass filter, we here restrict ourselves to a two-dimensional state vector, representing the horizontal position of the vehicle. Due to this restriction, we have to consider a simpler system than that in (1)–(3). To distinguish between variables in our system and filter models, we use asterisks for variables in the filter model. Our filter model reads, using the same delta notation as in (4)–(5),

$$\delta\mathbf{x}^*_k = \mathbf{x}^*_k - \tilde{\mathbf{x}}_k, \tag{6}$$

$$\begin{aligned}\delta\mathbf{x}^*_{k+1} &= \mathbf{x}^*_{k+1} - \tilde{\mathbf{x}}_{k+1} = \mathbf{x}^*_k + \mathbf{u}_k + \mathbf{v}^*_k - \tilde{\mathbf{x}}_k - \mathbf{u}_k \\ &= \delta\mathbf{x}^*_k + \mathbf{v}^*_k,\end{aligned}\tag{7}$$

$$\mathbf{z}_k = \mathbf{h}^*(\mathbf{x}^*_k) + \mathbf{w}^*_k = \mathbf{h}^*(\tilde{\mathbf{x}}_k + \delta\mathbf{x}^*_k) + \mathbf{w}^*_k, \tag{8}$$

with the assumptions

$$E\{\mathbf{v}^*_k\mathbf{v}^{*T}_l\} = \mathbf{Q}_k\delta_{kl}, \tag{9}$$

$$E\{\mathbf{w}^*_k\mathbf{w}^{*T}_l\} = \mathbf{R}_k\delta_{kl}, \tag{10}$$

where δ_{kl} denotes the Kronecker delta, such that the noise sequences are uncorrelated from time step to time step. We also need to specify the distributions of the noise sequences and the initial position offset, $\delta\mathbf{x}^*_0$. A convenient, but not necessary, assumption is to assume Gaussian distributions,

$$p(\delta\mathbf{x}^*_0) = \mathcal{N}(\mathbf{0}, \mathbf{P}_0), \tag{11}$$

$$p(\mathbf{v}^*_k) = \mathcal{N}(\mathbf{0}, \mathbf{Q}_k), \tag{12}$$

$$p(\mathbf{w}^*_k) = \mathcal{N}(\mathbf{0}, \mathbf{R}_k). \tag{13}$$

Equation (11) indicates that the initial position has a normal distribution centered around the position $\tilde{\mathbf{x}}_0$, given by the inertial navigation system. We further assume that the process noise, measurement noise and initial position are uncorrelated,

$$E\{\mathbf{v}^*_k\mathbf{w}^{*T}_l\} = \mathbf{0}, \tag{14}$$

$$E\{\mathbf{v}^*_k\mathbf{x}^{*T}_0\} = \mathbf{0}, \tag{15}$$

$$E\{\mathbf{w}^*_k\mathbf{x}^{*T}_0\} = \mathbf{0}, \tag{16}$$

for all k and l. The function $\mathbf{h}^*(\mathbf{x}^*_k)$ indicates the depth at position $\mathbf{x}^*_k$ given by the digital terrain map. We here use terrain maps consisting of gridded nodes, and the depth values given by $\mathbf{h}^*$ are found by bilinear interpolation of the terrain database. The noise sequence $\mathbf{w}^*_k$ in (8) therefore models both map noise (including interpolation errors) and the sensor noise. The measurement vector $\mathbf{z}_k$ consists of the total sea depths at the individual measurement footprints, computed as the sum of the AUV depth, given by a pressure sensor, and the measurements from the bathymetric sensor. The noise sequence $\mathbf{w}^*_k$ therefore contains contributions from map errors, pressure sensor noise and bathymetric sensor noise. For a detailed analysis of the depth accuracy for the HUGIN class AUVs, we refer to [9].

C. The Recursive Bayesian Filter Equations

Let $\mathbb{Z}_k$ be the augmented measurement vector consisting of all the measurements up to time step k. From Bayes' formula (see e.g. [11]) and our filter model, (6)-(8), we have

$$\begin{aligned} p(\delta\mathbf{x}_k^*|\mathbb{Z}_k) &= \frac{p(\mathbf{z}_k|\delta\mathbf{x}_k^*,\mathbb{Z}_{k-1})p(\delta\mathbf{x}_k^*|\mathbb{Z}_{k-1})}{p(\mathbf{z}_k|\mathbb{Z}_{k-1})} \qquad (17)\\ &= \frac{p_{\mathbf{w}_k^*}(\mathbf{z}_k-\mathbf{h}^*(\tilde{\mathbf{x}}_k+\delta\mathbf{x}_k^*))p(\delta\mathbf{x}_k^*|\mathbb{Z}_{k-1})}{\int_{\mathbb{R}^2} p_{\mathbf{w}_k^*}(\mathbf{z}_k-\mathbf{h}^*(\tilde{\mathbf{x}}_k+\delta\mathbf{x}_k^*))p(\delta\mathbf{x}_k^*|\mathbb{Z}_{k-1})\mathrm{d}\delta\mathbf{x}_k^*}. \end{aligned}$$

Our measurement update can then be written as

$$p(\delta\mathbf{x}_k^*|\mathbb{Z}_k) = \alpha^{-1}p_{\mathbf{w}_k^*}(\mathbf{z}_k-\mathbf{h}^*(\tilde{\mathbf{x}}_k+\delta\mathbf{x}_k^*))p(\delta\mathbf{x}_k^*|\mathbb{Z}_{k-1}), \quad (18)$$

where

$$\alpha = \int_{\mathbb{R}^2} p_{\mathbf{w}_k^*}(\mathbf{z}_k-\mathbf{h}^*(\tilde{\mathbf{x}}_k+\delta\mathbf{x}_k^*))p(\delta\mathbf{x}_k^*|\mathbb{Z}_{k-1})\mathrm{d}\delta\mathbf{x}_k^*. \quad (19)$$

The minimum square error (MMSE) estimate is then given by, see [11],

$$\delta\hat{\mathbf{x}}_k = E\{\delta\mathbf{x}_k^*|\mathbb{Z}_k\} = \int_{\mathbb{R}^2} \delta\mathbf{x}_k^* p(\delta\mathbf{x}_k^*|\mathbb{Z}_k)\mathrm{d}\delta\mathbf{x}_k^*, \quad (20)$$

with the estimated covariance matrix

$$\hat{\mathbf{P}}_k = \int_{\mathbb{R}^2} (\delta\mathbf{x}_k^*-\delta\hat{\mathbf{x}}_k^*)(\delta\mathbf{x}_k^*-\delta\hat{\mathbf{x}}_k^*)^T p(\delta\mathbf{x}_k^*|\mathbb{Z}_k)\mathrm{d}\delta\mathbf{x}_k^*. \quad (21)$$

For the time update of our position distribution we have, from conditioning on the position offset from the previous time step and using (7),

$$\begin{aligned} p(\delta\mathbf{x}_{k+1}^*|\mathbb{Z}_k) &= \int_{\mathbb{R}^2} p(\delta\mathbf{x}_{k+1}^*,\delta\mathbf{x}_k^*)\mathrm{d}\delta\mathbf{x}_k^*\\ &= \int_{\mathbb{R}^2} p(\delta\mathbf{x}_{k+1}^*|\mathbb{Z}_k)p(\delta\mathbf{x}_k^*|\mathbb{Z}_k)\mathrm{d}\delta\mathbf{x}_k^*\\ &= \int_{\mathbb{R}^2} p_{\mathbf{v}_k^*}(\delta\mathbf{x}_{k+1}^*-\delta\mathbf{x}_k^*)p(\delta\mathbf{x}_k^*|\mathbb{Z}_k)\mathrm{d}\delta\mathbf{x}_k^*. \quad (22) \end{aligned}$$

Given the distribution of the initial position, $p(\mathbf{x}_0^*)$, the equations (17) and (22) can now be used recursively to obtain the distribution of the position offsets for each time step. The integrals in the equations are, however, not analytically solvable, and we therefore need to evaluate these integrals numerically.

D. Point Mass and Particle Filters

The Point Mass and Particle Filters are numerical estimation methods for solving the optimal Bayesian filter equations (17) and (22). The formulation of PMF and the Bayesian bootstrap PF algorithms in the framework of terrain aided navigation can be found in [10], wherein it was also concluded that the PMF gives a more robust and stable terrain navigation solution. In the PMF, the probability distribution of the position offset is estimated using a grid of point masses. From the grid approximation, any type of estimate can be computed, including the maximum a posteriori (MAP) estimate and the mean of the posterior, i.e. the MMSE estimate, and its covariance. If the probability density is unimodal, the MAP and MMSE estimates in most cases coincide, whereas in multi modal probability densities the MAP estimate coincides with one of the modes, while the MMSE estimate is located somewhere between the modes. In the results presented herein, the MMSE estimates were used.

IV. The HUGIN Real-Time Terrain Navigation System

A. TerrP Plugin

Terrain navigation is now available as an additional navigation feature for all HUGIN vehicles. The HUGIN TerrP module is implemented as a plugin running on the payload processor. TerrP is integrated in the main navigation system in a loosely coupled manner. When the system is running, TerrP receives navigation data from NavP and bathymetry measurements from the selected sensor via CORBA interfaces. Primarily, the MBE should be used, but the system is also capable of using altitude data from the DVL [4] or even from the vehicle altimeters. The navigation and bathymetry data are used in the terrain navigation algorithm, together with the pre-loaded digital terrain model, to obtain a position fix that can be sent back to NavP. TerrP keeps processing the data recursively, until certain pre-defined convergence criteria are met. The most important convergence criterion is whether the computed posterior is single modal. This is important since NavP uses a Kalman filter which assumes Gaussian error models. If TerrP computes a multi modal posterior for the position estimate, the convergence criteria will not be met, and the estimate will not be sent to NavP. When the convergence criteria are met, it should be noted that the MMSE and MAP estimates normally coincide.

Whenever the TerrP estimate has converged, the estimate is sent to the integrity system, which performs additional tests on the estimate. If the tests are successful, the TerrP estimate is sent to NavP as an ordinary position measurement. Finally, NavP has its own wild-point filter that the TerrP estimate has to pass before eventually being used in the Kalman filter.

After convergence and subsequent integrity tests, a new terrain navigation sequence is started. The same happens if the convergence criteria are not met after a certain predefined number of measurements. As a consequence of this, all the

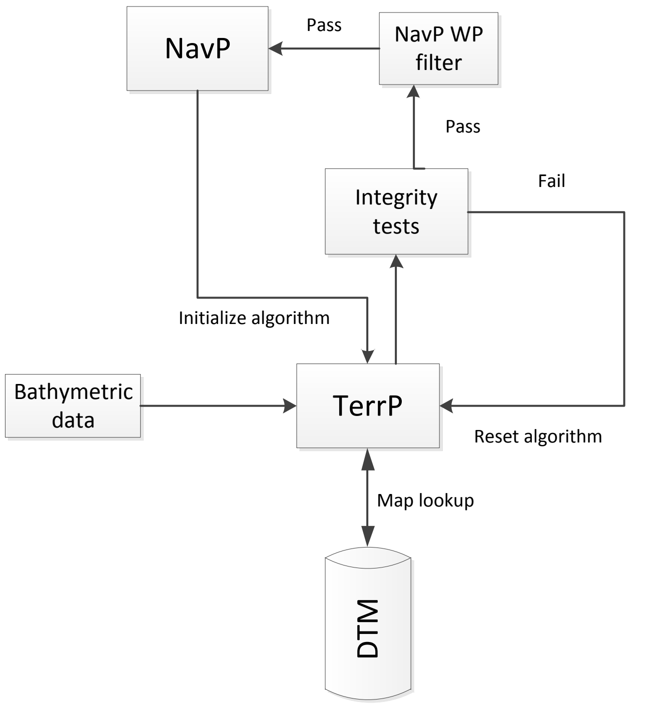

Fig. 4. Overview of TerrP data flow.

converged position estimates are based on different bathymetric data, minimizing the correlations between the updates. The data flow of the TerrP system is summarized in Fig. 4.

The current version of TerrP uses a 2-dimensional implementation of the PMF algorithm described in Section III. Possible depth bias effects, e.g. due to uncompensated tide levels, can be countered for through the use of relative profiles, as discussed in [10].

B. Integrity System

The integrity system of the TerrP module was briefly discussed in [12]. The integrity of a navigation system can be defined as its ability to provide timely warnings if and when it should not be used. In the loosely coupled approach which is used in the TerrP/NavP integration, it is crucial that as few as possible of the measurements sent to the NavP Kalman filter are inconsistent. Thus, the design goal of the integrity system has been to avoid Type II errors (accepting wrong position updates), even if this entails a lot of Type I errors (rejecting good updates). In the current version of the integrity system, three different integrity tests are used, one suitability of terrain test and two different goodness-of-fit tests for the estimated position. The terrain suitability test simply checks whether the standard deviation of the bottom measurements is above a pre-selected limit, indicating that there is enough variation in the terrain to obtain a good position estimate. The two goodness-of-fit tests check: i) the correlation between the measured depths (z) and the map depths at the estimated position (d), which should be close to 1, and ii) the relative standard deviation, defined as $\sigma(z-d)/\sigma(z)$, which should be much smaller than 1. The user has option of turning each of the three integrity tests on and off.

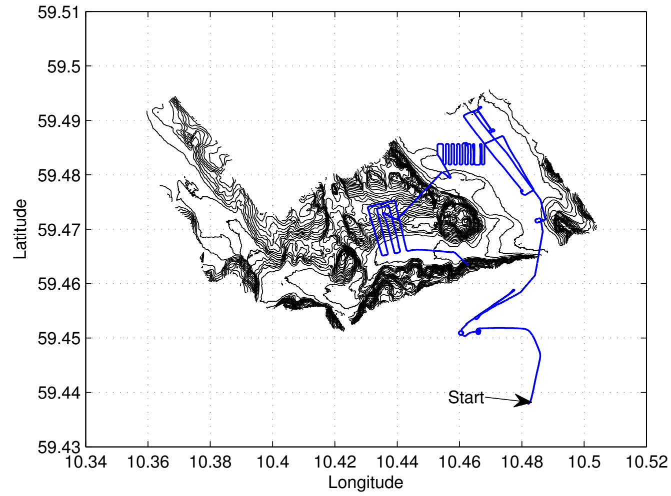

Fig. 5. Trajectory of test mission and terrain contours in the operation area.

C. Map Generation

The terrain navigation system requires a depth map of the operation area. This map should be uploaded to the HUGIN vehicle before the operation. TerrP uses a simple grid format, in which the sea depth at regular grid points are stored. The system uses bilinear interpolation when looking up the depths between the nodes. TerrP map files can be generated both from previous HUGIN missions and from external bathymetry surveys. Bathymetry data, from HUGIN or other sources, can be gridded and saved on the TerrP format by the Kongsberg Maritime *Reflection* post-mission analysis software package. Before the mission, the TerrP map files are uploaded to the vehicle using the TerrPOS interface.

As an alternative to using a pre-deployed depth map, TerrP also has the ability to create its own map during the mission. This map can be used for terrain navigation later on in the same mission. One way of using this functionality would be to map a small area using the TerrP map engine in the start of the mission, when the navigation accuracy is high. After the mapping stage, the vehicle continues its operation as it would normally do, before returning to the previously mapped area when the navigation accuracy has degraded, and a TerrP position fix is needed. The resulting accuracy of this fix will be bounded below by the navigation accuracy at the time of the map generation. This technique, called sequential mapping and navigation, is closely related to the well-known simultaneous localization and mapping (SLAM) problem [13], [14], and its use was demonstrated in [5].

V. SEA TRIAL RESULTS

TerrP has been tested in sea trials several times over the last few years, with a range of different bathymetric sensors. Results from tests with EM2000 MBE data were described in [5] and with DVL data in [4].

Here we present some new sew trial results from a HUGIN 1000 vehicle equipped with an EM2040 MBE. The sea trial was conducted outside Horten, Norway, in February 2013. This test was part of the Factory Acceptance Test (FAT) of a vehicle before delivery to its end customer, so the mission included testing of several other vehicle systems besides terrain navigation. Fig. 5 shows the entire mission trajectory, together with terrain contours of the area. The terrain navigation system was tested towards the end of the mission, as the vehicle left the relatively flat area in the northeastern part of the area and traveled towards an area with more terrain variations, known to be suitable for terrain navigation. During the entire mission, a surface vessel was following the vehicle, recording HiPAP (acoustic positioning) measurements of the vehicle position [15]. However, during the terrain navigation tests, the HiPAP measurements were not sent to the vehicle, leaving the terrain navigation as the only source of position updates. In post-processing the HiPAP measurements were used in the computation of a highly accurate reference solution, using the NavLab navigation software package [16]. During the terrain navigation test, DVL aiding to the INS was also turned off for shorter periods, to test the robustness of the terrain navigation system in cases of DVL outages. The map database used in this test was based on data from an EM1002 survey from a surface ship. The data was gridded to a 10 m horizontal resolution TerrP map, using the aforementioned Reflection software package. As a rule of thumb, a terrain navigation position accuracy comparable to the horizontal map resolution can be expected in suited terrain.

Fig. 6 shows an overview of all the estimated TerrP positions, together with the real-time (NavP) navigation trajectory, the reference (NavLab) trajectory and the HiPAP measurements. The red crosses indicate TerrP positions that converged according to the selected convergence criteria, but were rejected by the integrity system, whereas the black crosses are converged TerrP positions that were ultimately sent to NavP as position updates. The red dots are TerrP positions before convergence. Notice how all the converged TerrP positions in the flat area were rejected by the integrity system. In the rougher area, however, many of the converged TerrP fixes passed the integrity test, even though a large proportion of seemingly sound updates were still rejected, due to the conservative tuning of the integrity system. All in all, 59% of the converged TerrP fixes were rejected.

Fig. 7 shows the difference between the real-time navigation solution (NavP aided with TerrP) and the post-processed reference solution, together with the NavP estimated navigation accuracy. As the reference solution is the best possible navigation solution available, with an expected accuracy of 1–2 meters (1σ), this difference can be thought of as the actual error in the real-time navigation. In two periods (after approx. 210–237 minutes and 262–271 minutes), the DVL aiding was turned off. In the first period, it takes a while before a TerrP position is accepted, and the estimated navigation accuracy is quickly deteriorating. Then, when a TerrP position is accepted, both the actual navigation error and the estimation accuracy

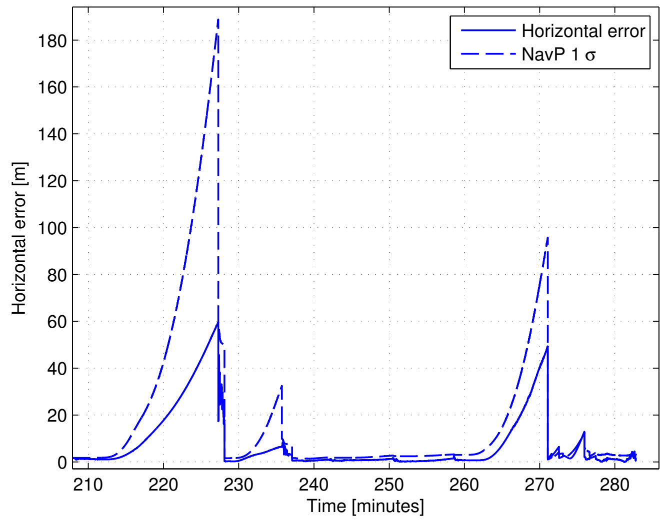

Fig. 7. Horizontal error in NavP during terrain navigation test.

is effectively reduced. The same happens again, towards the end of the first DVL outage. Then when the DVL aiding is turned on again, the error and estimated accuracy is further reduced. In the period between the DVL outages, both DVL and TerrP aiding is used, and the navigation error as well as the estimated uncertainty remains low (1 – 3 meters, 1σ). During the second DVL outage period, similar behavior as in the first outage period is seen.

To summarize, the results from this tests effectively show how TerrP aiding is able to maintain high navigation accuracy in suited terrain, as long as NavP is run with normal DVL aiding. In periods without DVL aiding, TerrP is able to bind the navigation accuracy to some extent, but due to the conservatively tuned integrity system the frequency of the accepted TerrP updates may be quite low, leading to high overall uncertainties between accepted updates. It should be noted, however, that the risk of DVL failure is low, and it was used here primarily to stress the TerrP system and investigate its robustness.

In a more realistic scenario, TerrP would be used as the sole position update source for much longer time periods than what was obtainable during this short test. As an example, the HUGIN 1000 HUS vehicle, owned and operated by FFI, successfully used terrain navigation as the only position update source during a transit of almost 7 hours (50 km) in the Barents sea in 2009, arriving in the target area with a navigation error of only 4 meters [12].

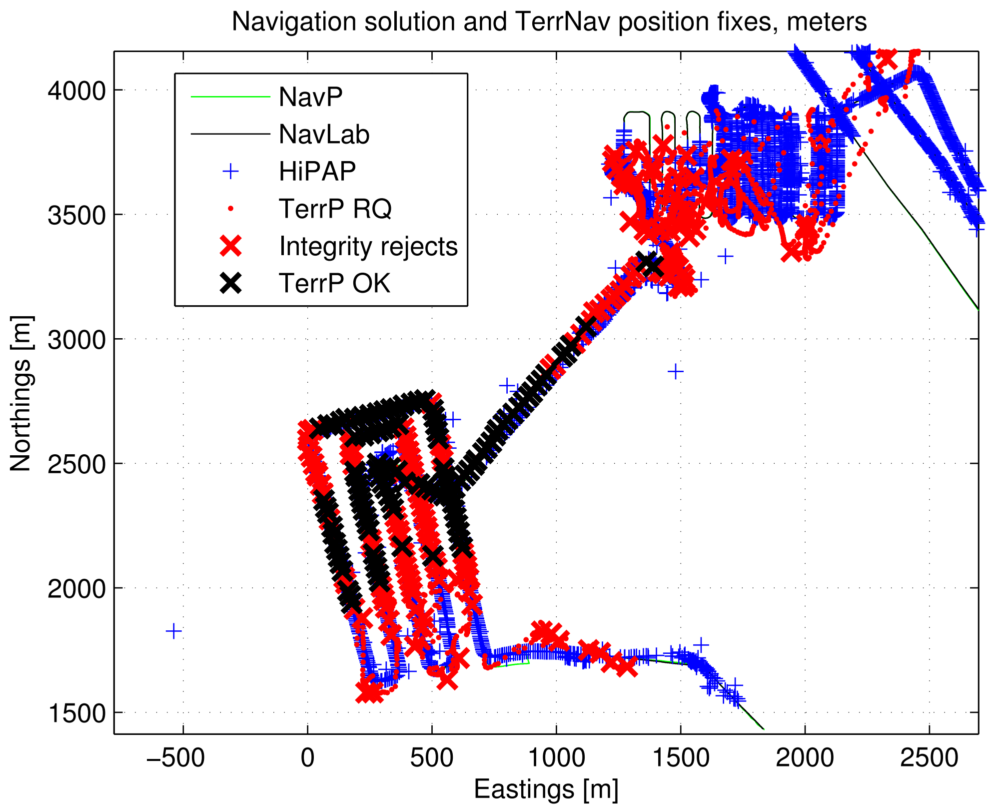

Fig. 6. Overview of vehicle trajectory and TerrP position fixes.

VI. Conclusions

This paper has given an overview of the HUGIN AUV terrain navigation module. The module is the result of several years of research at the Norwegian Defence Research Establishment (FFI) and has been successfully tested in several sea trials. A point mass filter (PMF) is used to estimate the probability density of the vehicle position based on bathymetric measurements, usually from a multibeam echo sounder (MBE) and a digital terrain model (map) of the operation area. The module has now been commercialized by Kongsberg Maritime as an optional module for the HUGIN navigation system and has been delivered to customers.

The terrain navigation module increases the autonomy of the vehicle, in that the vehicle is able to stay submerged throughout the operation, independent of GPS surface fixes or acoustic aiding from a mother ship. The system normally uses a pre-deployed map based on previous surveys, but it if a prior map does not exist, the system is able to build a map during the mission and later use this map for terrain navigation.

As an example of the performance of the system, sea trial results from a test with a HUGIN 1000 vehicle equipped with an EM2040 MBE were presented. During the test, the vehicle navigation accuracy was better than 5 meters during normal operation in suitable terrain. Robustness to Doppler velocity log (DVL) outages was also demonstrated.

The HUGIN terrain navigation module is subject to ongoing research and development. Special effort is put into improving the robustness of the system, for example by adjusting some of the parameters *in-situ*, according to varying environmental conditions.

References

[1] P. E. Hagen, Ø. Hegrenæs, B. Jalving, Ø. Midtgaard, M. Wiig, and O. K. Hagen, *Underwater Vehicles*. Vienna, Austria: In-Tech Education and Publishing, 2009, ch. Making AUVs Truly Autonomous, pp. 129–152.

[2] Ø. Hegrenæs, “Autonomous navigation for underwater vehicles,” Ph.D. dissertation, Norwegian Unversity of Science and Technology, 2010, ISSN 1503-8181; 2010:101, 2010.

[3] B. Jalving, M. Mandt, O. K. Hagen, and F. Pøhner, “Terrain referenced navigation of AUVs and submarines using multibeam echo sounders,” in *Proceedings of the UDT Europe 2004*, Nice, France, 2004.

[4] K. B. Ånonsen and O. K. Hagen, “An analysis of real-time terrain aided navigation results from a HUGIN AUV.” in *Proceedings of the IEEE/ION Oceans 2010 Conference*, Seattle, WA, September 2010.

[5] ——, “Recent developments in the HUGIN AUV terrain navigation system,” in *Proceedings of the MTS/IEEE Oceans Conference 2011*, Kona, HI, USA, September 2011.

[6] B. Jalving, K. Gade, O. K. Hagen, and K. Vestgård, “A toolbox of aiding techniques for the HUGIN AUV integrated inertial navigation system,” in *Proceedings of the IEEE Oceans 2003*, San Diego, CA, 2003.

[7] P. E. Hagen and J. Kristensen, “The HUGIN AUV "plug and play" payload system,” in *Proc. Oceans 2002*, Biloxi, MS, USA, October 2002.

[8] Ø. Hegrenæs, K. Gade, O. K. Hagen, and P. E. Hagen, “Underwater transponder positioning and navigation,” in *Proceedings of the MTS/IEEE Oceans Conference*, Biloxi, MS, October 2009.

[9] B. Jalving, “Depth accuracy in seabed mapping with underwater vehicles,” in *Proceedings of the IEEE Oceans ’99*, Seattle, WA, 1999.

[10] K. B. Ånonsen and O. Hallingstad, "Terrain aided underwater navigation using point mass and particle filters," in *Proceedings of the IEEE/ION Position Location and Navigation Symposium (PLANS) 2006*, San Diego, CA, April 2006.
[11] Y. Bar-Shalom, X. Li, and T. Kirubarajan, *Estimation with Applications to Tracking and Navigation*. New York: John Wiley & Sons, 2001.
[12] O. K. Hagen, K. B. Ånonsen, and M. Mandt, "The HUGIN real-time terrain navigation system," in *Proceedings of the MTS/IEEE Oceans 2010 Conference*, Seattle, WA, USA, September 2010.
[13] T. Bailey and H. Durrant-Whyte, "Simultaneous localization and mapping (SLAM): Part II State of the art," *IEEE Robotics & Automation Magazine*, vol. 13, no. 3, pp. 108–117, Sep. 2006.
[14] H. Durrant-Whyte and T. Bailey, "Simultaneous localization and mapping (SLAM): Part I The essential algorithms," *IEEE Robotics & Automation Magazine*, vol. 13, no. 2, pp. 99–110, Jun. 2006.
[15] Kongsberg Maritime AS, "High precision acoustic positioning – HiPAP," Product brochure, available online at www.km.kongsberg.com, 2013.
[16] K. Gade, "NavLab, a generic simulation and post-processing tool for navigation," *European Journal of Navigation*, vol. 2, no. 4, pp. 51–59, November 2004. [Online]. Available: www.navlab.net